Eur J Cancer Clin Oncol, Vol. 21, No. 1, pp. 85–96, 1985.
Printed in Great Britain.

0277-5379/85$3.00+0.00

Organization of Cytoskeleton and Fibronectin Matrix in Rous Sarcoma Virus (RSV)-transformed Fibroblast Lines with Different Metastatic Potential*

MARIA FLAVIA DI RENZO,† GUIDO TARONE,‡ PAOLO M. COMOGLIO‡ and PIER CARLO MARCHISIO‡§

†*Institute of Human Anatomy and* ‡*Institute of Histology and General Embryology, University of Turin, Turin, Italy*

Abstract—*Metastatic clones growing in 0.6% 'hard' agar were selected from the non-metastatic Rous sarcoma virus (RSV)-transformed tumorigenic B77-3T3 mouse fibroblast line. The incidence of spontaneous lung metastases varied among clones around 100%, while it was lower than 5% in the parental tumor line. The organization of microfilaments, microtubules and intermediate filaments as well as the pattern of extracellular fibronectin matrix were analyzed by immunofluorescence in two representative clones (B77-AA6 and B77-AA12) and was compared with the structural features displayed by a highly metastasizing RSV-induced mouse sarcoma line (SR-BALB). In the metastatic clones studied microtubules and intermediate filaments were similarly organized in a pattern not significantly different from that of the non-metastatic parental cell line. The major finding was a marked concentration of actin-containing structures in the periphery of cells and notably at the level of surface protrusions, suggesting a high surface motility. In the same lines the production of fibronectin and its distribution in the cell layer and culture medium were analyzed. Metabolic labelling and immunofluorescence experiments indicated that the nonmetastasizing cells (B77-3T3) retain higher amounts of fibronectin in the cell layer and organize this molecule in extracellular fibers, while the metastatic clones (B77-AA6 and B77-AA12) as well as the metastatic line (SR-BALB) are unable to retain and organize fibronectin at their surface. This paper shows that the progression of tumorigenic cell lines toward a metastatic phenotype involves a redistribution of cytoskeletal actin and a loss of organized fibronectin matrix.*

INTRODUCTION

TUMOR metastasis is a sequential multistep process whereby the cells are actively released from the primary tumor and disseminate to distant organs where they proliferate to form new tumor foci (for reviews see [1–3]).

Critical stages of the metastasis process—such as the invasion of tissues surrounding primary tumor including the intravascular compartment, dissemination to and arrest in the capillary bed of distant organs, reaching once again the extravascular compartment—must involve marked alterations in cell shape, morphology, motility and adhesiveness. These latter properties are controlled by the cytoskeleton and by the interactions of cells with their extracellular matrix and are known to be altered in transformed cells [4–6].

In this paper the organization of some proteins forming cytoskeletal networks and the extracellular matrix is described by immunofluorescence microscopy in RSV-transformed fibroblasts with different metastatic potential. The model studied offers some unique advantages since it is based on cells sharing the same origin

Accepted 28 June 1984.
*This work has been supported by the Italian National Research Council (C.N.R.), Progetto Finalizzato Controllo della Crescita Neoplastica.
§To whom requests for reprints should be addressed.

and transformed by a known v-oncogene (*v-src*). Four lines are employed: (a) the non-transformed 3T3 fibroblast-like line; (b) the B77-3T3 line, obtained by transforming *in vivo* the 3T3 line [7]; this line expresses the *v-src* gene, produces enzymatically active *pp60src*, is tumorigenic, but does not metastasize [8]; (c) the highly metastasizing B77-AA6 and B77-AAl2 clones isolated in 'hard' agar from the above B77-3T3 line [8]; these clones stably retain their metastatic potential as well as their growth and morphological characteristics during *in vitro* propagation [9]; and (d) the SR-BALB line, obtained by transforming *in vitro* BALB/c fibroblasts with the SR-D strain of the RSV [10]; this line spontaneously displays a high metastatic capability [8].

MATERIALS AND METHODS

Cell culture and cloning in agar

The BALB/3T3 line—a mouse non-transformed fibroblast-like line—was obtained from the Americal Type Culture Collection. The non-metastasizing B77-3T3 cell line, kindly provided by Dr J. M. Bishop, University of California, San Francisco, CA, is a clone of BALB/c 3T3 fibroblasts transformed *in vitro* by the Bratislava 77 Strain of Rous sarcoma virus [7]. The metastasizing SR-BALB cell line, kindly provided by Dr J. T. Parsons, University of Virginia, Charlottesville, VA, was obtained by injecting chicken fibroblasts transformed by Schmidt-Ruppin D strain of the RSV in BALB/c mice [10]. The metastasizing B77-AAl2 and B77-AA6 lines are subclones of the B77-3T3 line, isolated in our laboratory [8, 9] by cloning in 0.6% agar. The metastatic potential of the four transformed and tumorigenic lines was previously assessed [8, 9]. The BALB/c 3T3, B77-3T3, B77-AA6, B77-AAl2 and SR-BALB lines were routinely cultured in Dulbecco's modified Eagle's medium (DMEM) supplemented with 10% fetal calf serum and antibiotics. The M4 and M9 mouse sarcoma lines were kindly provided by Dr Mantovani, Istituto Mario Negri, Milan, Italy, and grown as described [11].

Cloning efficiency in 0.6% ('hard') agar was measured as previously described [8] by seeding cells in agar at the concentrations of 2×10 cells per 60-mm diameter plastic dish. Briefly, on an underlayer (4 ml) of 0.6% Difco Noble agar in DMEM plus 10% fetal calf serum, 10% tryptose phosphate broth and antibiotics, single cells were plated suspended in a top layer (1.5 ml) of 0.6% agar in the same medium. All cultures were carried out in quadruplicate. Twenty-one days later, colonies visible to the naked eye were counted with the aid of a millimeter grid and microscopically checked.

Spontaneous lung metastasis

The production of spontaneous lung metastases was assayed by subcutaneous (s.c.) injection in the abdominal flank of syngeneic mice [12] of tumor cells grown *in vitro*. Subconfluent cultures were incubated with 0.25% trypsin–0.02% EDTA for 10 min at 37°C; reaction was blocked by adding complete medium; cells were collected at 800 rpm, extensively washed and resuspended in medium without serum. Cell viability was not affected by this treatment, as assessed by evaluation of plating efficiency.

Immediately after spontaneous death, treated mice were subjected to autopsy and metastases were counted under a dissecting microscope.

Antisera to fibronectin and cytoskeletal proteins

The antiserum to affinity chromatography-purified human plasma fibronectin was prepared as previously described [13]. Its specificity for mouse fibronectin was earlier demonstrated by immunoprecipitation experiments [14].

The antisera to tubulin and actin were raised by immunizing rabbits against homogeneous calf brain tubulin free of microtubule-associated proteins and chicken gizzard actin respectively. The immunization protocol followed published procedures [15, 16]. The rabbit antibody to rat vimentin was prepared using sodium dodecyl sulfate-denatured antigen [17, 18]. Vinculin antiserum was a kind gift of Dr D. Drenckhahn, Marburg, F.R.G.; this antiserum was found to recognize vinculin from several mammalian species [19, 20]. Fluorescein isothiocyanate-labeled goat anti-rabbit IgGs were purchased from Kirkegaard and Perry, Gaithersburg, MD, U.S.A.

Quantitation of fibronectin

Metabolic labeling of proteins was achieved by incubating cell monolayers for 5 hr with 20 μC/ml of [^{35}S]-methionine (800 Ci/mmol, Amersham) in methionine-free medium containing 5% fetal calf serum.

Quantitative immunoprecipitation of labeled soluble fibronectin was performed as previously described [14]. Cell-associated fibronectin was solubilized by extracting cells with the Triton–DOC–SDS buffer (20 mM Tris–HCl, pH 7.4, 150 mM NaCl, 0.5% Triton X-100, 0.5% sodium desoxycholate, 0.1% sodium dodecyl sulfate, 5 mM ethylendiamine tetra-acetic acid and 2 mM phenylmethylsulfonyl fluoride as protease inhibitor). The extracts were sonicated to reduce viscosity and centrifuged in an Eppendorf

microfuge for 15 min. The solubilized material was incubated with an excess of antiserum for 1 hr at 0°C, and immunocomplexes were recovered by adsorption on Protein A–Sepharose beads (Pharmacia). All the fibronectin present in the solution was immunoprecipitated under these conditions, as tested by a second immunoprecipitation cycle on the supernatant of the Protein A–Sepharose incubation. Immunoprecipitated fibronectin was separated in sodium dodecylsulfate polyacrylamide gel electrophoresis (SDS-PAGE) according to Laemmli [21]; the protein band was excised from the gel and the associated radioactivity was measured by liquid scintillation counting.

Immunofluorescence microscopy

Cells were grown to subconfluent monolayers on glass coverslips, rinsed with PBS and fixed with 3.7% paraformaldehyde in PBS for 10 min at room temperature. After washing with PBS containing 0.2% bovine serum albumin, fixed cells were incubated for 60 min with rabbit antiserum to fibronectin diluted 1/50 followed by a FITC-labeled goat anti-rabbit IgG. For the detection of intracellular antigens, formaldehyde fixation was followed by a 2-min extraction at room temperature with PBS containing 0.2% Triton X-100. After rinsing, coverslips were incubated sequentially in the primary and secondary antibodies for 45 min at 37°C. Coverslips were then mounted in 50% glycerol in PBS and examined in a Leitz Dialux microscope equipped with an epi-illumination system or in a Leitz Diavert inverted microscope equipped both with epifluorescence and interference reflection optics. Fluorescence pictures were recorded on Kodak Tri-X films while IRM pictures were taken on Agfa Ortho 25 films.

Scanning electron microscopy

Scanning electron microscopy (SEM) was performed by Dr C. De Giuli Institute of Pharmacology, University of Milan, Italy, as follows. Coverslip-attached cells were fixed in 2.5% glutaraldehyde in PBS for 1 hr at room temperature, rinsed and dehydrated in graded ethanol, followed by infiltration with amyl acetate and critical-point drying. After gold coating, cells were observed in a Cambridge Stereoscan electron microscope and pictures recorded on Polaroid plates.

RESULTS

In this paper we have tried to correlate cell structural features with the ability of RSV-transformed lines to produce metastases, by simultaneously analyzing their spontaneous metastatic capability and their patterns of cytoskeletal organization and fibronectin matrix.

Spontaneous metastasis and cloning efficiency in agar

Spontaneous metastatic potential was assayed in syngeneic mice injected subcutaneously with tumorigenic doses of B77-3T3, B77-AA6 or SR-BALB cells. As the animals spontaneously died, metastases were scored at autopsy.

As shown in Table 1, B77-3T3 tumors did not produce metastases in a significant number of animals; among 50 mice, only two developed pulmonary metastases. SR-BALB tumors gave spontaneous lung metastases in 13/14 injected animals. Metastases became detectable in animals surviving more than 6 weeks; at this time they were scored with the aid of a dissecting microscope. Metastatic nodules were observed only in the lung.

Since a direct correlation was found between metastatic ability and cloning efficiency in 'hard' agar of RSV-transformed fibroblasts [8], clones of B77-3T3 cells growing in 'hard' agar were selected and their behavior was tested *in vitro* and *in vivo* [9]. They showed metastastic abilities and cloning efficiency in agar comparable to that of the metastasizing SR-BALB line. In Table 1 the behavior of the B77-AA6 clone employed in the present study is shown.

Table 1. *Cloning efficiency in 'hard' agar and spontaneous lung metastases (MTS) of an RSV-transformed cell line*

Cell line	Cloning efficiency (%)	Incidence†	Average No. of MTS ± S.D.	Mean survival times ± S.D.
B77-3T3	0.05	2/50	2 ± 1	43 ± 8
B77-AA6	9.85	13/14	5 ± 1	49 ± 12
SR-BALB	10.90	11/13	6 ± 2	60 ± 17

*Mice were injected subcutaneously in the abdominal flank with 1×10^5 cells *in vitro* grown B77-3T3 or B77-AA6 cells and with 1×10^5 or 5×10^5 cells *in vitro* grown SR-BALB cells.

†No. of mice bearing metastases/No. of mice bearing tumor; the difference between the incidence were significant at $P < 0.001$ (χ^2 test).

Cell morphology and cytoskeleton organization

Indirect immunofluorescence microscopy and specific antibodies were employed to study the organization of cytoskeletal networks in control non-transfomed 3T3 fibroblasts and in four transformed cell lines equipped with different metastatic capabilities (SR-BALB, B77-3T3, B77-AA6 and B77-AA12). In Fig. 1 the organization of cytoplasmic microtubules is described. No significant difference in the overall distribution of microtubule arrays was found among transformed cell lines. When the latter were compared to their non-transformed counterpart (3T3 cells) it was found that transformed cells displayed a higher density of microtubules (Fig. 1b–d), which was probably due to the more rounded morphology of the cells as compared to flattened control cells (Fig. 1a). A major difference which appeared in transformed cells was the constant absence of the primary cilium which conversely was consistently found in 3T3 cells (Fig. 1a, arrowhead). Whether this observation is meaningful or not remains to be established. The distribution of intermediate filaments of the vimentin type (not shown) was fairly similar to the general pattern of microtubules in accordance to data reported elsewhere for other cell types [22].

The organization of microfilaments displayed by control non-transformed 3T3 cells was essentially based on stress fibers running close to the substratum-attached side (Fig. 2a). This pattern was greatly altered in all transformed cells as reported for most transformed cell types [4, 5] and stress fibers mostly disappeared in RSV-transformed cells (Fig. 2b–d).

In B77-3T3 non-metastasizing tumorigenic cells a moderate preservation of microfilament bundles, running close to the ventral membrane and mostly in the flattened outer rim, was observed by careful focusing (Fig. 2c, arrow). However, the density of this fibrous pattern was very irregular. It should also be noted that non-metastasizing B77-3T3 cells show a marked tendency to form clusters and to keep close cell-to-cell contacts long before reaching confluency (Figs 1c and 2c). This pattern was never observed in cells which showed high tendency to metastasize (SR-BALB, B77-AA6 and B77-AA12), which conversely tended to grow isolated and to form cell-to-cell contacts only when reaching confluency. The detection of organized microfilament bundles occurs only occasionally in these latter cells and actin seldom appears in organized bundles. On the contrary, in these cells actin is mostly associated with the peripheral rim of cytoplasm and notably within a rich complement of peripheral protrusions appearing in the form of long microvilli and ruffles. Such a difference is also documented by pictures obtained by SEM (Fig. 3). The peripheral distribution of actin-containing structures suggests that metastasizing cell lines are provided with higher membrane motility and probably also with higher migratory activity on the substratum.

The adhesive properties of non-transformed 3T3 cells and those of the RSV-transformed lines were compared by a study of vinculin distribution at adhesion plaques and of the relative distance between the ventral membrane and the substratum, carried out by interference reflection microscopy (IRM). The location and the number of focal and close contacts are different in non-transformed and transformed cells only from a quantitative point of view (not shown). No significant alterations in the shape of adhesion systems upon transformation, as reported in other transformed cell types [6, 23], can be appreciated in these mouse lines. No difference was found between lines with different metastatic potential (not shown). The observations made on B77-AA6 cells were almost identically reproduced in B77-AA12 cells, a sister high-metastasizing clone of the same B77-3T3 cell line.

Synthesis and organization of fibronectin

The organization of fibronectin in the extracellular matrix was studied by indirect immunofluorescence using specific rabbit antibodies. As shown in Fig. 4 (a and b), control non-transformed cells (3T3) organize an extensive fibronectin matrix. Transformed, non-metastatic, B77-3T3 cells partially retained the ability to organize fibronectin and displayed short fibrillary structures localized at the ventral cell surface or connecting adjacent cells (Fig. 4c). In the metastatic lines (B77-AA6, B77-AA12 and SR-BALB) fibrillary structures were missing (Fig. 4d–f) and fibronectin appeared in the form of a weak dotted surface staining. The difference in fibronectin staining pattern was common to two other sarcoma lines with low (M9) and high (M4) metastatic properties [11] (Fig. 4g and h), suggesting that the lack of fibronectin organization is a rather general feature of metastatic cells growing *in vitro*.

This difference might be due to alteration of either fibronectin synthesis or deposition in the extracellular matrix. To discriminate between these two possibilities, synthesis and accumulation of fibronectin were measured by metabolic labeling and immunoprecipitation of the radioactive molecule (see Materials and Methods for details). All transformed cell lines produced two- to five-fold less fibronectin than non-transformed 3T3 cells (Table 2). No further reduction was

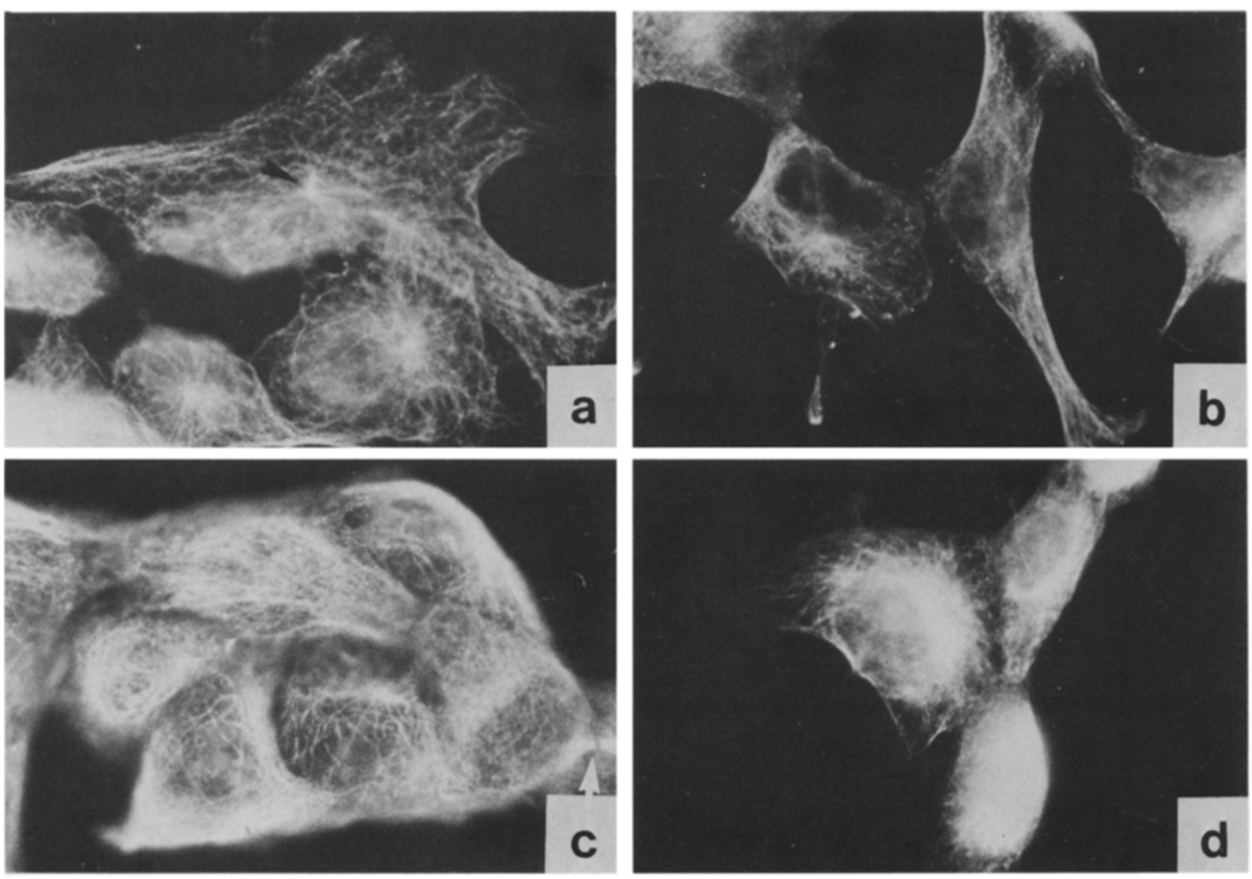

Fig. 1. Immunofluorescence staining of microtubules with tubulin antibodies in control 3T3 fibroblasts (a) and in RSV-transformed fibroblasts (b–d). Panel c shows transformed tumorigenic B77-3T3 cells equipped with low-metastasizing capability while cells with high-metastasizing capability are shown in panels b (SR-BALB) and d (B77-AA6). The display of cytoplasmic microtubules is not significantly different in normal vs transformed cell types except for the presence of primary cilia in 3T3 cells (e.g. black arrowhead in a). Note that B77-3T3 cells tend to grow in clusters and often microtubule-containing intercellular bridges are preserved (e.g. white arrow in c). Magnification, ×2300.

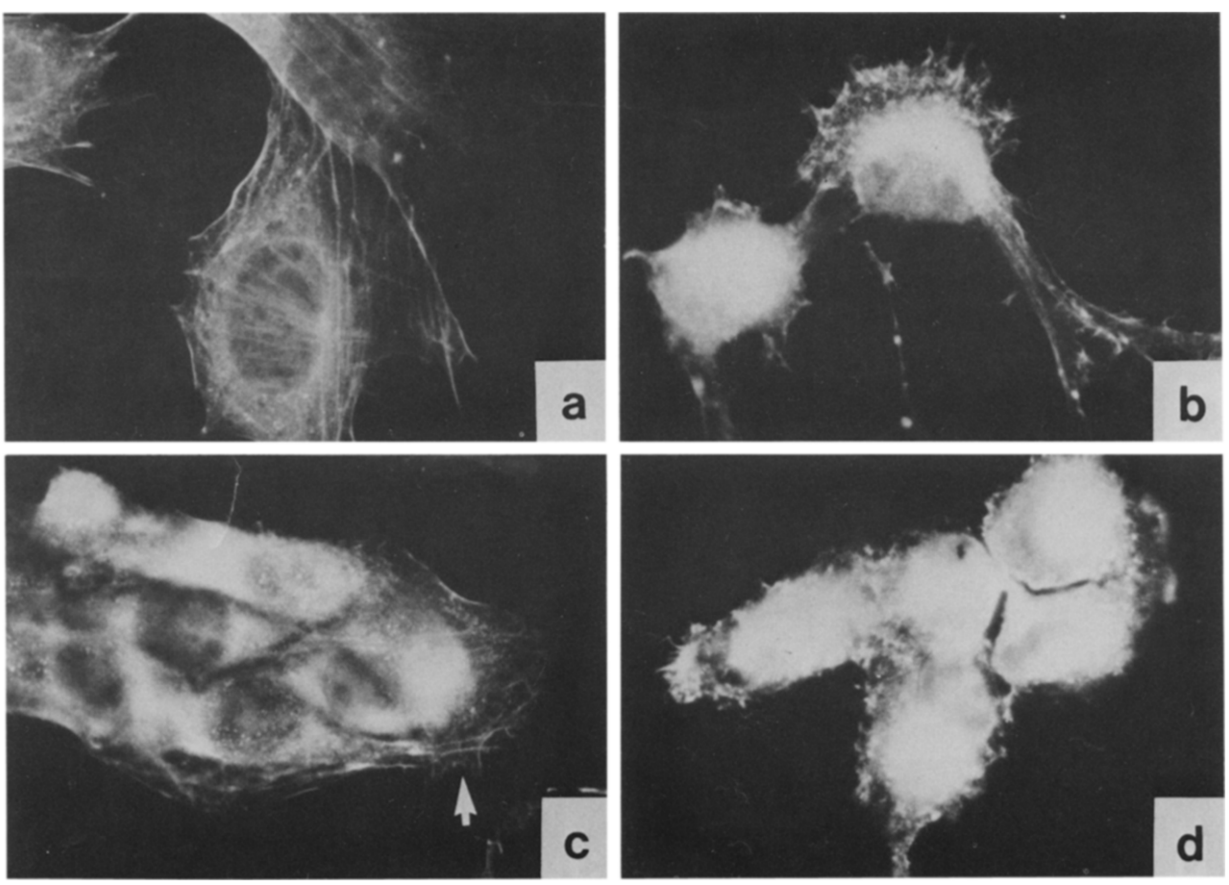

Fig. 2. Immunofluorescence staining of actin-containing stuctures with actin antibodies in control 3T3 fibroblasts (a) and in RSV-transformed fibroblasts (b–d). Panels represent the same cell types as in Fig. 1. Actin is mostly organized as stress fibers in control 3T3 cells (a). Low-metastasizing B77-3T3 cells show a moderate preservation of thin microfilament bundles (c, at white arrow) while high-metastasizing SR-BALB (b) and B77-AA6 (d) show actin predominantly associated with peripheral cell protrusions. Magnificantion, ×2300.

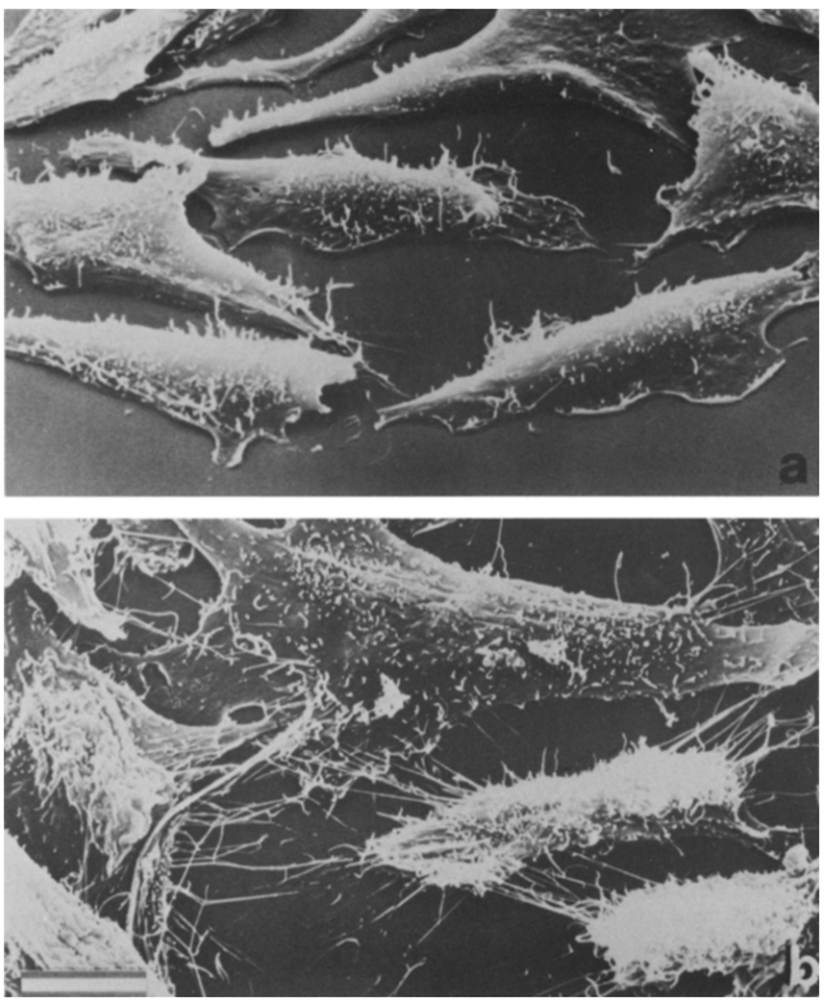

Fig. 3. Scanning electron microscopy pictures of tumorigenic low-metastasizing B77-3T3 cells (a) and their derived high-metastasizing B77-AA6 clone (b). The main difference between the two cell types is the great number of surface protrusions observed in B77-AA6 cells in the form of microvilli and membrane ruffles. Bar denotes 10 μm.

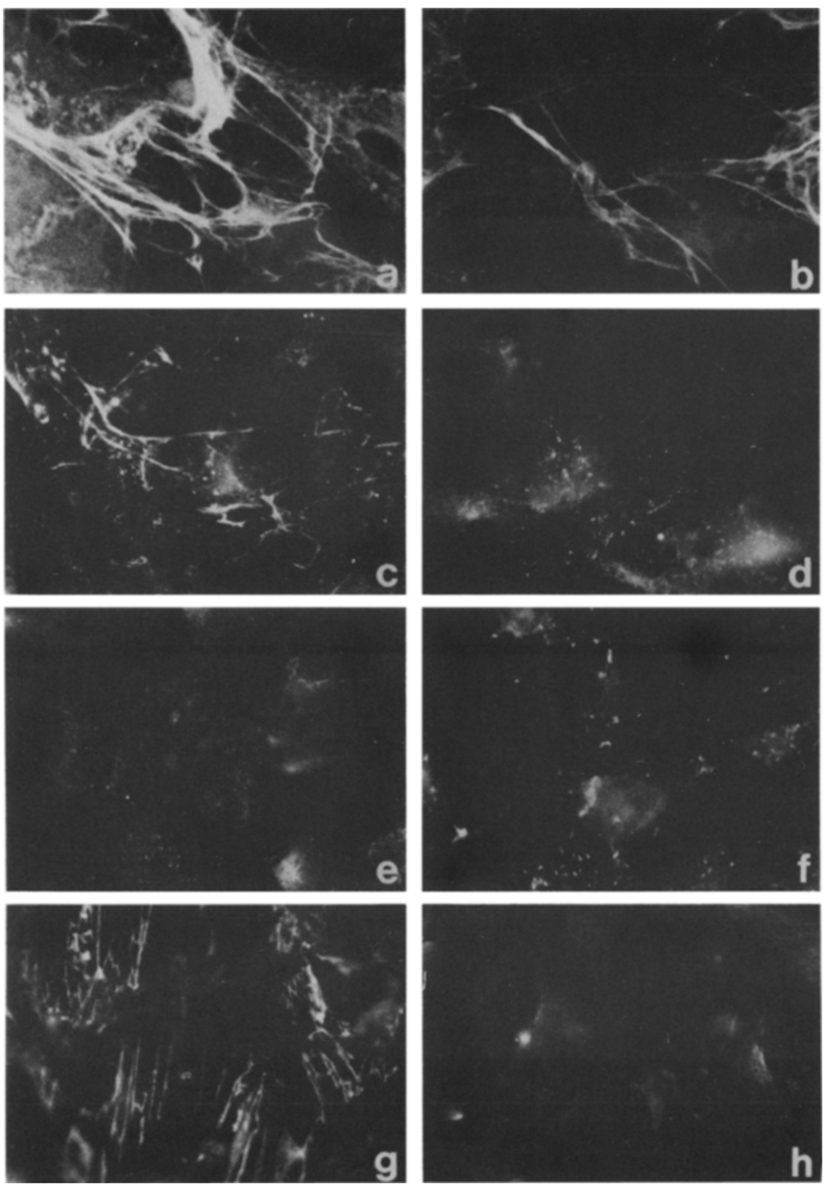

Fig. 4. Immunofluoresence staining of fibronectin in control 3T3 (a and b) and malignant fibroblasts (c–h). Fibronectin is organized in thick extracellular fibrils in control 3T3 cells (a, b). Low-metastasizing B77-3T3 cells (c) display reduced amounts of fibronectin organized in fibrillar structures. A similar pattern is also present in a different cell line (M9) with low-metastatic properties (g). High-metastasizing SR-BALB (f) and (h) cell lines and B77-AA 6(d) and B77-AA12 (e) clones do not organize fibronectin in extracellular structures and display only a dotted surface pattern. Magnification, ×2300.

observed in metastasizing cells that synthesized and accumulated amounts of fibronectin identical (B77-AA6 and B77-AA12) or higher (SR-BALB) than non-metastasizing cells (B77-3T3) (Table 2). When the relative distribution of fibronectin between the culture medium and the cell layer was analyzed, it was found that metastatic lines (SR-BALB, B77-AA6 and B77-AA12) retained a lower proportion of fibronectin in the cell layer than the non-metastatic B77-3T3 cells (Table 2), confirming the immunofluorescence results.

In conclusion, these data clearly indicate that these metastatic cells fail to organize secreted fibronectin even in a simple adhesive pericellular matrix.

DISCUSSION

Cells able to metastasize must be equipped with the ability to actively detach from the primary tumor mass, to migrate through vessel walls and to establish cell-to-substratum and cell-to-cell contacts. These processes depend on cell deformability, motility and adhesiveness. The cytoskeleton regulates these functions by determining cell shape and locomotion and by the transmembrane control over the cell surface organization and interaction with the extracellular matrix. Dramatic reduction and/or disorganization of microfilament networks, matrix components and membrane proteins were found to accompany neoplastic transformation [4–6, 24].

The extent to which tumor cells establish metastases has been correlated with cell shape modulation and adhesiveness alterations [25–30]. Interesting but fragmentary data have been reported about specific alterations of cytoskeleton, extracellular matrix and membrane components associated with the metastatic phenotype [29–35].

The opportunity to reconsider this problem stemmed from the isolation of cellular clones provided with high-metastasizing potential, derived from a cell line, RSV-transformed, which was nearly devoid of such potential. The biological and molecular features of RSV-transformed cells are well known insofar as the *v-src* oncogene—responsible for transformation—and its *pp60src* transforming product have been thoroughly investigated [36–39]. The lines studied here offer some unique possibilities. First, the opportunity of comparison of metastatic and non-metastatic lines with their non-transformed counterparts. This enables us to show that the non-metastatic but tumorigenic and anchorage-independent B77-3T3 line possesses a fully transformed phenotype and that differences between metastatic and non-metastatic lines are not attributable to a partial reversion to the normal phenotype. In this view, it is also noteworthy that the non-metastatic line is stably clonal and that all lines exhibit stable metastatic or non-metastatic behavior after long-term propagation *in vitro* [8, 9]. This excludes that the observed differences between metastatic and non-metastatic cells are due to tumor heterogeneity. In addition, the non-metastatic transformed B77-3T3 line may also be compared with a fibroblast line (SR-BALB) of the same inbred species, transformed by a different strain of the same virus, that spontaneously, i.e. without being selected, exhibits a high metastatic potential [8]. The similarity of the phenotypes observed in B77-AA6 and SR-BALB lines excludes that differences between the parental B77-3T3 line and its clones selected in agar are only due to the random selection by the same sort of pressure of two non-related phenotypes (morphologic and metastatic).

In this paper we have considered and compared the cytoskeletal and matrix organization of these RSV-transformed lines, which differ only in their malignancy, viz. their ability to produce metastases in syngeneic animals. The main finding is that microfilaments and the extracellular fibronectin matrix are the cellular

Table 2. Synthesis and distribution of fibronectin in non-metastatic and metastatic cell lines

Cell line*	Total†	Medium†	Cell layer†	% in cell layer‡
3T3	6200	2480	3720	60
B77-3T3	1320	920	400	30
B77-AA6	1450	1131	319	22
SR-BALB	3520	2830	770	21

*Cells were grown to confluency and pulsed for 5 hr with [^{35}S]-methionine. Fibronectin was immunoprecipitated with specific antibodies from either the culture medium or the cell extracts as described in Materials and Methods. After separation by electrophoresis, the fibronectin band was located by fluorography and cut from the gel to evaluate associated radioactivity.

†cpm per 2×10^6 cells. All experiments were made in triplicate and numbers represent the mean value.

‡Percentage of total cpm.

structures which are more deeply affected in metastasizing cells.

The conclusion we offer is that the general distribution of microtubules and intermediate filaments in metastasizing lines appears slightly changed only because these cells undergo an overall change in shape, becoming more rounded and generally more detached from the substratum. This conclusion is in agreement with the more general problem of the cytoskeleton of transformed cells [40]. The major differences between low- and high-metastasizing lines is the redistribution of intracellular actin and its noticeable association with the peripheral rim in metastasizing cells. This concentration of actin at the cell periphery is also accounted for by a concomitant increase of surface activity in the form of protrusions of various types. This finding supports also the idea that high-metastasizing cells are provided with higher motile activity and tend to support more active locomotion movements. Another finding which should be pointed out is that low-metastasizing B77-3T3 cells show a much more marked tendency to grow in epithelial-like sheets and to keep tight cell-to-cell contacts. The opposite is apparent for the high-metastasizing cell lines (including the clone B77-AA6 derived from the low-metastasizing B77-3T3 line), which tend to grow as isolated elements reciprocally contacting only with their own peripheral protrusions.

We also studied the synthesis and deposition of fibronectin, a glycoprotein of the extracellular matrix known to be involved in cell adhesion and motility (for reviews see [41–43]). Although neoplastic transformation is accompanied by a considerable decrease in fibronectin matrix, our results show that non-metastatic cells still retain the ability to assemble fibronectin in thin extracellular fibrils. All metastatic lines tested fail to organize this molecule at their surface. Different mechanisms have been implied in the reduction of fibronectin levels upon neoplastic transformation [42]. The further reduction of fibronectin in metastatic cells can tentatively be ascribed to secretion of proteolytic enzymes that specifically digest matrix components. In fact it has been shown that the SR-BALB and B77-AA6 lines release high levels of collagenase [44] as well as hyaluronic acid and heparan sulfate-degrading enzymes [Cappelletti and Ricoveri, personal communication]. Collagens and proteoglycans interact with fibronectin and control the assembly of fibronectin in the extracellular matrix (for review see [43]).

A transmembrane interaction between fibronectin and actin is known to occur and to be important in the control of cell adhesion and motility [45]. It is interesting to note that in the metastatic cells we examined the lack of fibronectin organization corresponds to a rearrangement of actin but not of other cytoskeletal elements. Thus it is reasonable to suppose that an alteration of one or more components of the transmembrane complex linking extracellular matrix and intracellular cytoskeleton may be relevant for the acquisition of the metastatic phenotype.

Acknowledgements—The skillful technical assistance of Ms M. R. Amedeo and Ms P. Rossino is gratefully acknowledged. We thank Dr C. De Giuli Morghen, Institute of Pharmacology, University of Milan, for providing SEM pictures.

REFERENCES

1. Fidler IJ, Gersten DM, Hart IR. The biology of cancer invasion and metastasis. *Adv Cancer Res* 1978, **28**, 149–250.
2. Poste G, Fidler IJ. The pathogenesis of cancer metastasis. *Nature* 1980, **283**, 139-146.
3 Liotta LA, Hart IR. *Tumor Invasion and Metastasis.* The Hague, Martinus Nijhoff, 1982.
4. Edelman GM, Yahara I. Temperature-sensitive changes in surface modulating assemblies of fibroblasts transformed by mutants of Rous sarcoma virus. *Proc Natl Acad Sci USA* 1976, **73**, 2047–2051.
5. Wang E, Goldberg AR. Changes in microfilament organization and surface topography upon transformation of chick embryo fibroblasts with Rous sarcoma virus. *Proc Natl Acad Sci USA* 1976, **73**, 4065–4069.
6. David-Pfeuty T, Singer SJ. Altered distribution of the cytoskeletal proteins vinculin and alpha-actinin in cultured fibroblasts transformed by Rous Sarcoma virus. *Proc Natl Acad Sci USA* 1980, **77**, 6687–6691.
7. Bishop JM, Weiss SR, Oppermann H *et al.* The strategy of retrovirus gene expression. In: Barlati S, De Giuli Morghen C, eds. *Avian RNA Tumor Viruses.* Padova, Piccin, 1978, 181–189.
8. Di Renzo MF, Bretti S. Characterization of stable spontaneous metastatic variant line of RSV-transformed mouse fibroblasts. *Int J Cancer* 1982, **30**, 751–757.

9. Di Renzo MF, Doneda L, Larizza L, Comoglio PM. Metastatic clones selected from an RSV-induced mouse sarcoma share a common marker chromosome. *Int J Cancer* 1983, **31**, 455–461.
10. Parsons SJ, Riley SC, Mullen EE *et al.* Immune response to the *src* gene product in mice bearing tumors induced by injection of avian sarcoma virus-transformed mouse cells. *J Virol* 1979, **32**, 40–46.
11. Giavazzi R, Alessandri G, Spreafico F, Garattini S, Mantovani A. Metastasizing capacity of tumor cells from spontaneous metastases of transplantated murine tumors. *Br J Cancer* 1980, **42**, 464–472.
12. Stackpole CW. Distinct lung-colonizing and lung-metastasizing cell populations in B-16 mouse melanoma. *Nature* 1981, **289**, 788–800.
13. Tarone G, Amedeo MR, Di Renzo MF, Comoglio PM. Monoclonal antibodies to the collagen binding domain of human plasma fibronectin. *Exp Cell Biol* 1984, **52**, 225-236
14. Tarone G, Ceschi P, Prat M, Comoglio PM. Transformation sensitive protein with molecular weight of 45,000 secreted by mouse fibroblasts. *Cancer Res* 1981, **41**, 3648–3651.
15. Weber K, Rathke PC, Osborn M, Franke WW. Distribution of actin and tubulin in cells and in glycerinated cell models after treatment with cytochalasin B (CB). *Exp Cell Res* 1976, **102**, 285–297.
16. Weber K, Wehland J, Herzog W. Griseofulvin interacts with microtubules both *in vivo* and *in vitro*. *J Mol Biol* 1976, **102**, 817–829.
17. Osborn M, Weber K. The detergent-resistant cytoskeleton of tissue culture cells includes the nucleus and the microfilament bundles. *Exp Cell Res* 1977, **106**, 339–349.
18. Franke WW, Schmid E, Osborn M, Weber K. Intermediate-sized filaments of human endothelial cells. *J Cell Biol* 1979, **81**, 570–580.
19. Drenckhahn D, Mannherz HG. Distribution of actin and actin-associated proteins myosin, tropomyosin, alpha-actinin, vinculin, and villin in rat and bovine exocrine glands. *Eur J Cell Biol* 1983, **30**, 167–176.
20. Comoglio PM, Di Renzo MF, Tarone G, Giancotti F, Naldini L, Marchisio PC. Detection of phosphotyrosine containing proteins in the detergent insoluble cell fraction of RSV transformed fibroblasts by azobenzene phosphonate antibodies. *EMBO J* 1984, **3**, 483–489.
21. Laemmli UK. Cleavage of structural proteins during the assembly of the head of the bacteriophage T. *Nature* 1970, **227**, 680–683.
22. Geiger B, Singer SJ. Association of microtubules and intermediate filaments in chicken gizzard cells as detected by double immunofluorescence. *Proc Natl Acad Sci USA* 1980, **77**, 4769–4773.
23. Shriver K, Rohrschneider L. Organization of *pp60src* and selected cytoskeletal proteins within adhesion plaques and junctions of Rous sarcoma virus-transformed rat cells. *J Cell Biol* 1981, **89**, 525–535.
24. Marchisio PC, Capasso O, Nitsch L, Cancedda R, Gionti E. Cytoskeleton and adhesion patterns of cultured chick embryo chondrocytes during cell spreading and Rous sarcoma virus transformation. *Exp Cell Res* 1984, **151**, 332–343.
25. Nicolson GL, Winkelhake JL. Organ specificity of blood-borne tumor metastasis determined by cell adhesion. *Nature* 1975, **255**, 230–232.
26. Kramer RH, Nicolson GL. Interactions of tumor cells with vascular endothelial cell monolayers: a model for metastatic invasion. *Proc Natl Acad Sci USA* 1979, **76**, 5704–5708.
27. Murray JC, Liotta L, Rennard SI, Martin G. Adhesion characteristics of murine metastatic and nonmetastatic tumor cells *in vitro*. *Cancer Res* 1980, **40**, 347–350.
28. Raz A, Ben-Ze'ev A. Growth control and cell spreading: differential response in preneoplastic and in metastatic variants. *Int J Cancer* 1982, **29**, 711–715.
29. Raz A, Ben-Ze'ev A. Modulation of the metastatic capability in B16 melanoma by cell shape. *Science* 1983, **221**, 1307–1310.
30. Terranova VP, Liotta LA, Russo RG, Martin GR. Role of laminin in the attachment and metastasis of murine tumor cells. *Cancer Res* 1982, **42**, 2265–2269.
31. Hart IR, Raz A, Fidler IJ. Effect of cytoskeleton-disrupting agents on the metastatic behavior of melanoma cells. *JNCI* 1980, **64**, 891–898.
32. Raz A, Geiger B. Altered organization of cell-substrate contacts and membrane-associated cytoskeleton in tumor cell variants exhibiting different metastatic capabilities. *Cancer Res* 1982, **42**, 5183–5186.

33. Rieber M, Rieber MS. Metastatic potential correlates with cell-surface protein alterations in B16 melanoma variants. *Nature* 1981, **293**, 74–76.
34. Yogeeswaran G, Salk PL. Metastatic potential is positively correlated with cell surface sialylation of cultured murine tumor cell lines. *Science* 1981, **212**, 1514-1516.
35. Lotan R, Raz A. Low colony formation *in vivo* and in culture as exhibited by metastatic melanoma cells selected for reduced homotypic aggregation. *Cancer Res* 1983, **43**, 2088–2093.
36. Brugge JS, Erikson RL. Identification of a transformation specific antigen induced by an avian sarcoma virus. *Nature* 1977, **269**, 346–348.
37. Hanafusa H. Cell transformation by RNA tumor viruses. In: Fraenkel H, Wagner RP, eds. *Comprehensive Virology*. New York, Plenum Press, 1977, Vol. 10, 401–483.
38. Czernilofsky AP, Levinson AD, Varmus HE, Tischer E, Goodman HM. Nucleotide sequence of an avian sarcoma virus oncogene (*src*) and proposed amino acid sequence for gene product. *Nature* 1980, **287**, 198–203.
39. Hunter T, Sefton BM. The transforming gene product of Rous sarcoma virus phosphorylates tyrosine. *Proc Natl Acad Sci USA* 1980, **77**, 1311–1315.
40. Osborn M, Weber K. The display of microtubules in transformed cells. *Cell* 1977, **12**, 561–571.
41. Vaheri A, Mosher DF. High molecular weight, cell surface-associated glycoprotein (fibronectin) lost in malignant transformation. *Biochim Biophys Acta* 1978, **516**, 1–25.
42. Yamada KM, Olden K. Fibronectin-adhesive glycoproteins of the cell surface and blood. *Nature* 1978, **275**, 179–184.
43. Hynes RO, Yamada KM. Fibronectins: multifunctional modular glycoproteins. *J Cell Biol* 1982, **95**, 369–377.
44. Liotta LA, Thorgeirsson UP, Garbisa S. Role of collagenases in tumor cell invasion. *Cancer Met Rev* 1982, **1**, 277–288.
45. Singer II, Paradiso PR. A transmembrane relationship between fibronectin and vinculin (130 Kd protein): serum modulation in normal and transformed hamster fibroblasts. *Cell* 1981, **24**, 481–492.